Hindawi
Complexity
Volume 2021, Article ID 5578339, 9 pages
https://doi.org/10.1155/2021/5578339

Research Article

Basin of Attraction Analysis of New Memristor-Based Fractional-Order Chaotic System

Long Ding,[1] Li Cui ,[1] Fei Yu ,[2] and Jie Jin[1]

[1]*Hunan University of Science and Technology, Xiangtan, Hunan 411201, China*
[2]*School of Computer and Communication Engineering, Changsha University of Science and Technology, Changsha 410114, China*

Correspondence should be addressed to Li Cui; 348640501@qq.com

Received 7 February 2021; Revised 27 March 2021; Accepted 7 April 2021; Published 14 April 2021

Academic Editor: Guillermo Huerta Cuellar

Memristor is the fourth basic electronic element discovered in addition to resistor, capacitor, and inductor. It is a nonlinear gadget with memory features which can be used for realizing chaotic, memory, neural network, and other similar circuits and systems. In this paper, a novel memristor-based fractional-order chaotic system is presented, and this chaotic system is taken as an example to analyze its dynamic characteristics. First, we used Adomian algorithm to solve the proposed fractional-order chaotic system and yield a chaotic phase diagram. Then, we examined the Lyapunov exponent spectrum, bifurcation, SE complexity, and basin of attraction of this system. We used the resulting Lyapunov exponent to describe the state of the basin of attraction of this fractional-order chaotic system. As the local minimum point of Lyapunov exponential function is the stable point in phase space, when this stable point in phase space comes into the lowest region of the basin of attraction, the solution of the chaotic system is yielded. In the analysis, we yielded the solution of the system equation with the same method used to solve the local minimum of Lyapunov exponential function. Our system analysis also revealed the multistability of this system.

1. Introduction

Recently, chaotic systems have attracted wide attention from researchers due to their own particularities and their vast application potential in the memristor [1–4], random number generator [5, 6], secure communication [7–9], image encryption [10–14], and artificial neural network [15–20]. How to increase the complexity of a chaotic system and generate complex chaotic attractors to make it hard to encipher information in encryption system applications has become a field of interest for researchers both in and outside China. In 1971, Professor Shaotang Cai published the "Memristor-The Missing Circuit Element" [21]. After theoretic derivation of the relationships between the four basic electrical physical quantities—voltage, current, charge, and magnetic flux—Cai assumed that there exists a fourth basic circuit element: the memristor. Over the most recent decade, the use of memristors in designing chaotic circuits, such as pure memristor networks and complex circuits containing one or more memristors, has been extensively studied [22–24]. Results show that memristor-based chaotic circuits provide a greater variety of dynamic behaviors. As memristors are nanoelements which are not commercialized yet, in the current studies related to conventional memristor-based chaotic circuits, researchers tend to use existing simulation analog elements to realize a memristor analog circuit and then use it to investigate the dynamic properties of the designed system. For this reason, selecting a memristor model and designing a memristor analog circuit constitutes an important part of fundamental research.

At present, the generation and application of multistability and extreme multistability has become a very hot topic for chaotic circuit systems [25–29]. Compared with other chaotic systems, combining memristors with chaotic systems can generate chaotic attractors possessing complicated dynamic properties. Yet the multistability of a chaotic system is dependent on the initial state of the system.

In fact, a multistable dynamic system usually has a very complicated basin of attraction structure that can be defined by a fractal boundary. From a mathematical point of view, a basin of attraction indicates that there is a chaotic attractor on the smooth hypercurve observed in a dynamic system showing invariables and a subspace with positive finite time fluctuation in addition to the invariable subspace in asymptotic termination state. Although the chaotic attractor is laterally stable, the insertion of an unstable periodic orbit in the chaotic attractor constitutes the source of losing this lateral stability. Whether the chaotic attractor will lose lateral stability is determined by how the orbit becomes unstable. Dynamically, beyond invariable manifolds, there can appear different bifurcations and different forms of basin of attraction. If there are sieve basins in a multistable chaotic system, their final state will be totally unpredictable. This is similar to a random process, for which only the probability of the final state of the system can be determined.

The purpose of this research is to take the analysis on the proposed chaotic system as an example to exhibit the nonlinear dynamical behavior of a memristor-based fractional-order chaotic system and to provide a new theoretical basis for the study of nonlinear systems. In the study, we used Adomian algorithm to solve the proposed fractional-order chaotic system and yield the chaotic phase diagram, and the bifurcation, Lyapunov exponent, and SE complexity of the chaotic system. Here, we specifically present a new analytical method of using Lyapunov exponent to describe the state of the basin of attraction of a chaotic system, from which we yielded the solution, basin of attraction region, transitional region, and divergence trajectory of the system. Our system analysis also revealed the multistability of the system.

2. New memristor-Based Fractional-Order Chaotic System

We propose a new memristor-based fractional-order chaotic system which is expressed by

$$\begin{cases} \dfrac{dx^q}{d^q t} = A(y - x), \\ \dfrac{dy^q}{d^q t} = Bx - xz - xW(w), \\ \dfrac{dz^q}{d^q t} = x^2 - Cz, \\ \dfrac{dw^q}{d^q t} = x. \end{cases} \tag{1}$$

The function of memristor [30] is

$$W(w) = 0.1w^2 + 0.6. \tag{2}$$

When $A = 5$, $B = 20$, $C = 4$, $q = 0.98$ $(0 < q < 1)$, and the initial value is (0.1, 0.1, 0.1, 0.1), Adomian decomposition algorithm is used to solve system (1) and yield the corresponding system phase diagram, as shown in Figure 1. When $q = 0.9$, the phase diagram of system (1) is as shown in Figure 2. Here, we are going to analyze the proposed fractional-order chaotic attractor subsystems for orders 0.98 and 0.9. Figure 2 is more complex than Figure 1.

2.1. Equilibrium Point and Lyapunov Exponent Analysis. The equilibrium points of system (1) can be obtained by solving the following equation:

$$\begin{cases} 0 = A(y - x), \\ 0 = Bx - xz - xW(w), \\ 0 = x^2 - Cz, \\ 0 = x. \end{cases} \tag{3}$$

Through equation (3), we get the equilibrium point for system (1) as (0, 0, 0, 0). When $q = 0.98$, the Lyapunov exponents of system (1) are LE1 = 0.7505, LE2 = −0.0297, LE3 = −0.2298, and LE4 = −9.8612, suggesting that system (1) is a chaotic system. The Lyapunov exponent of the system (1) is calculated and the corresponding index map is obtained based on predictor-corrector (PECE) method of Adams–Bashforth–Moulton type and Wolf's method. The Lyapunov exponents are shown in Figure 3.

2.2. Bifurcation and Lyapunov Exponent Spectrum Analysis. Assume that the fractional-order parameters are $q = 0.98$, $B = 20$, and $C = 4$; the control parameter A of system (1) is increased from 1 to 6; the initial value of system (1) is (0.1, 0.1, 0.1, 0.1); the step size of A is 0.01. The bifurcation diagram of the fractional-order system is as shown in Figure 4(a). We can see that when the fractional-order system is in order 0.98, system (1) is in the chaotic state. When parameters $q = 0.9$, $B = 20$, and $C = 4$ and again when control parameter A is increased from 1 to 6, the fractional-order system will come into the chaotic state through period doubling bifurcation. The bifurcation diagram is as shown in Figure 5(a) when the fractional-order parameters are $q = 0.98$, $A = 5$, and $C = 4$, the control parameter B of system (1) is increased from 10 to 22, the initial value of system (1) is (0.1, 0.1, 0.1, 0.1), and the step size of B is 0.01. The bifurcation diagram of the fractional-order system is as shown in Figure 6(a). We can see that when the fractional-order system is in order 0.98, system (1) will come into chaotic state through bifurcation. When parameters $q = 0.9$, $A = 5$, and $C = 4$ and again when control parameter B is increased from 10 to 22, the fractional-order system has hidden bifurcation. The bifurcation diagram is as shown in Figure 7(a). At the same time, the Lyapunov exponent of system (1) is calculated and the corresponding index map is obtained based on the predictor-corrector (PECE) method of Adams–Bashforth–Moulton type and Wolf's method. The Lyapunov exponents are as shown in Figures 4(b), 5(b), 6(b), and 7(b). The Lyapunov spectrum provides the parameter range when system (1) is in chaos, and these ranges are consistent with bifurcation analysis results.

2.3. SE Complexity Analysis. The complexity analysis of systems covers a range of fields. Researchers into these fields have reported different understandings about the complexity of the systems. So far, no consensus has been reached over the definition of complexity. The complexity of a

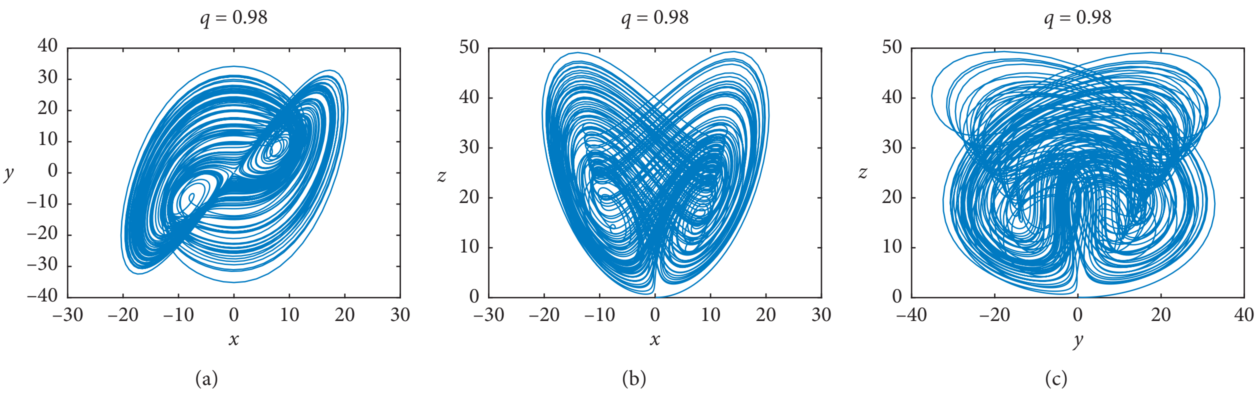

FIGURE 1: The chaotic attractor of system (1) with $q = 0.98$. (a) x-y plane, (b) x-z plane, and (c) y-z plane.

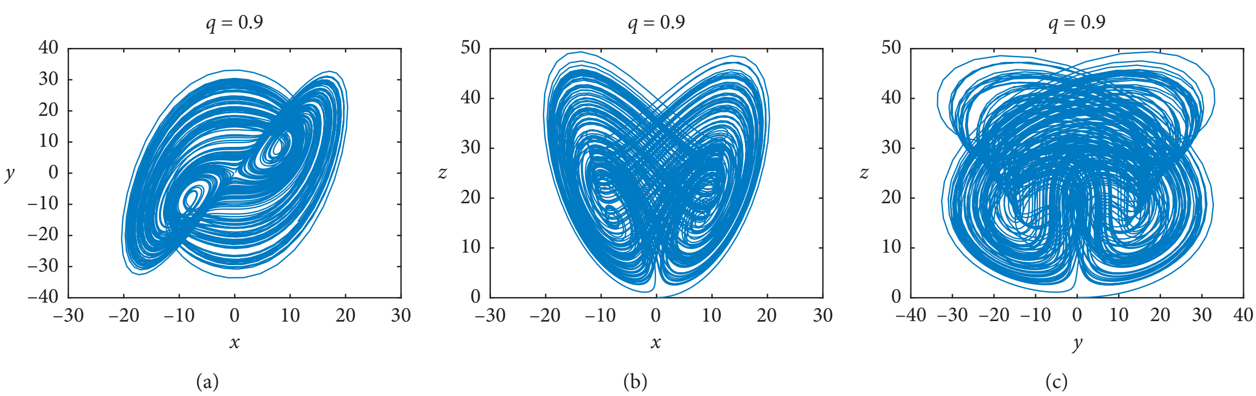

FIGURE 2: The chaotic attractor of system (1) with $q = 0.9$. (a) x-y plane, (b) x-z plane, and (c) y-z plane.

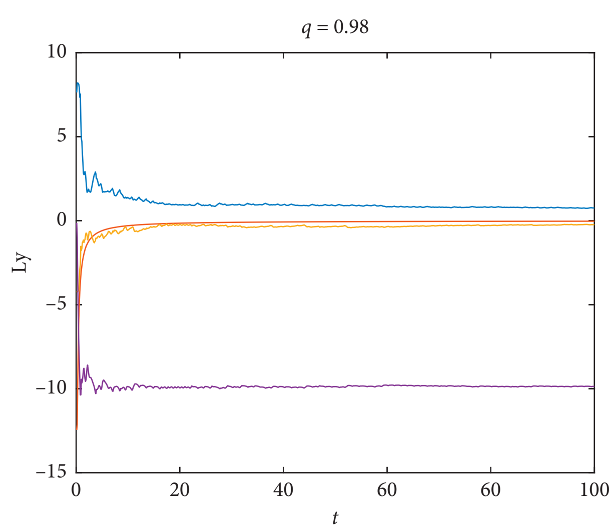

FIGURE 3: The Lyapunov exponents of system (1) with $q = 0.98$.

chaotic system is the random nature of the chaotic sequence. The higher the complexity of a chaotic system is, the closer the sequence is to a random one and, accordingly, the higher the security of the corresponding system becomes. The complexity of a chaotic system is essentially the complexity of chaotic dynamics. So far, many complexity algorithms have been used to measure the complexity of a system, such as multiscale entropy [31], Shannon entropy [32], fuzzy

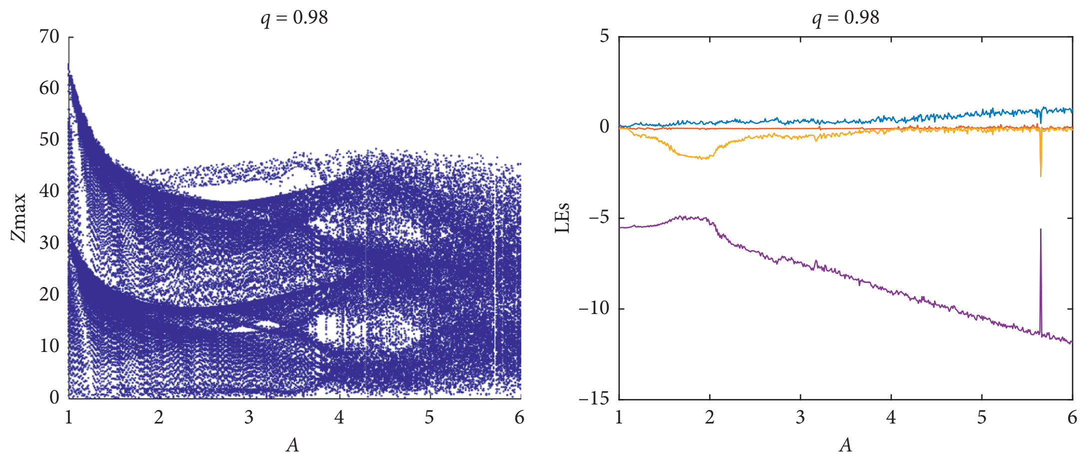

(a) (b)

Figure 4: (a) Bifurcation diagram of parameter A of system (1) with $q = 0.98$; (b) Lyapunov exponent spectrum of parameter A of system (1) with $q = 0.98$.

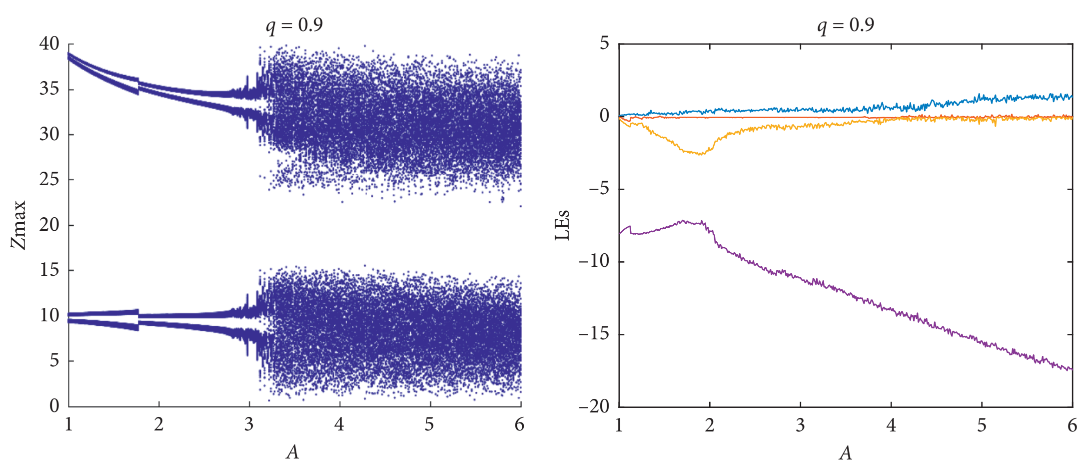

(a) (b)

Figure 5: (a) Bifurcation diagram of parameter A of system (1) with $q = 0.9$; (b) Lyapunov exponent spectrum of parameter A of system (1) with $q = 0.9$.

entropy [33], and spectral entropy (SE) [34]. Compared with other algorithms, SE is more popular for having fewer parameters and higher accuracy. For this reason, we used SE to measure the complexity of our new chaotic system. Furthermore, chaotic mapping-based SE can provide better basis for choosing the right parameters in real applications. Figure 8 shows the SE complexity analysis related to parameter A and order q. From this diagram, we can see that the lower the order is, the darker the color is and, accordingly, the greater the complexity of the system becomes. This well agrees with the reality that the lower the order of a fractional-order chaotic system, the greater the complexity of the chaos. Within the corresponding parameters, if this system is used in a chaotic secure communication system, the confidentiality of the communication system will be improved.

2.4. Basin of Attraction Analysis. Regarding fractional-order chaotic systems, we have published two articles on basin of attraction analysis [35, 36]. In the present study, we further analyzed the characteristics of a basin of attraction and again analyzed the stability of the system by considering Lyapunov exponential function. When the system operates in the initial state, it will move towards the direction in which Lyapunov exponential function decreases until reaching its local minima. The local minima point of Lyapunov exponential function means the stable point in phase space, where each attractor will surround a substantial basin of attraction. In that sense, these points are also called attractors. These basins of attraction represent a stable chaotic state. When the stable point comes into the lowest region of the basin of attraction, the solution of the chaotic system can be yielded. The size of a basin of attraction, as indicated by the radius of attraction, can be defined

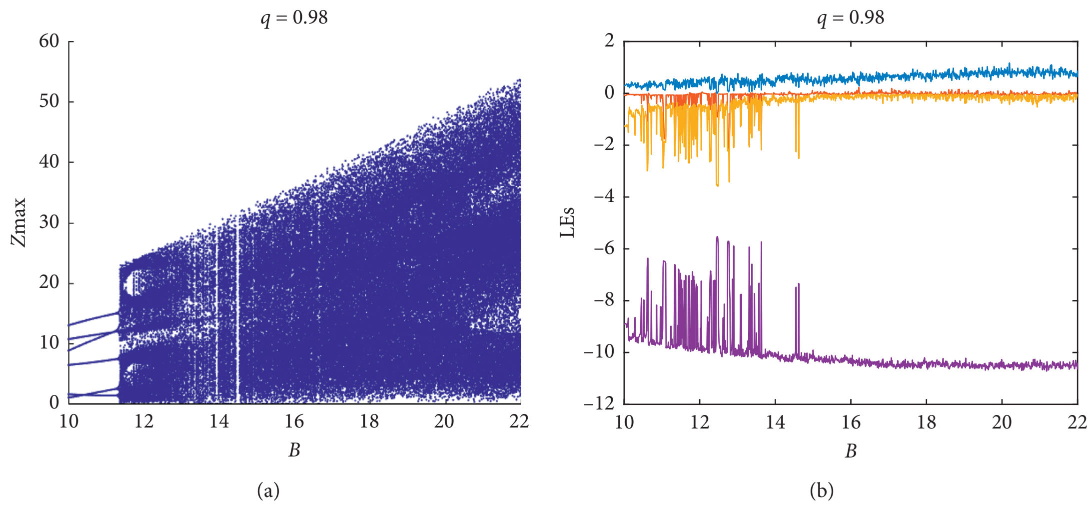

FIGURE 6: (a) Bifurcation diagram of parameter B of system (1) with $q = 0.98$; (b) Lyapunov exponent spectrum of parameter B of system (1) with $q = 0.98$.

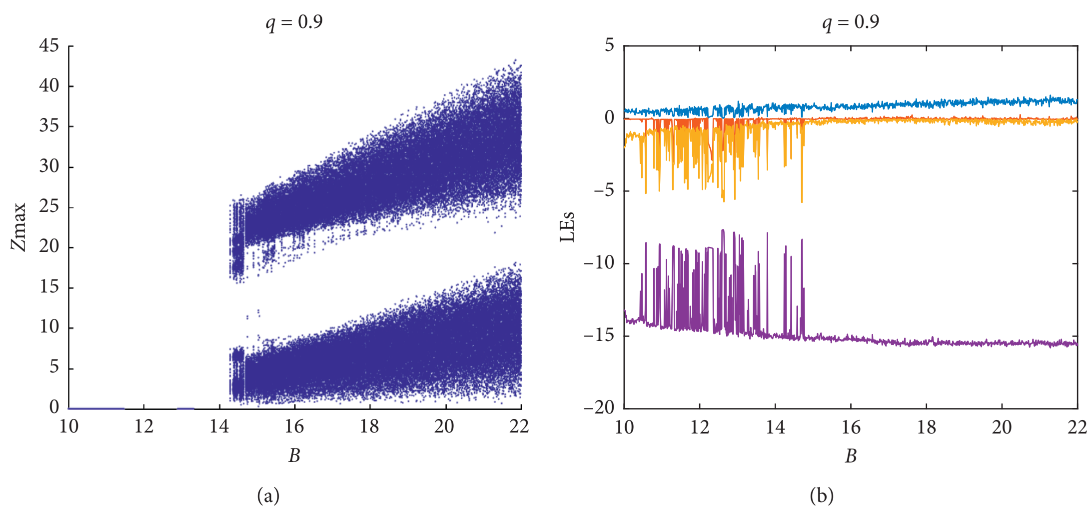

FIGURE 7: (a) Bifurcation diagram of parameter B of system (1) with $q = 0.9$; (b) Lyapunov exponent spectrum of parameter B of system (1) with $q = 0.9$.

as the maximum distance between all states contained in a basin of attraction or the maximum distance of the state that can be attracted by the attractor. In a dynamic system with more than one attractor, the corresponding basin may have a fractal boundary or even more complicated structure. Hence, in system (1), the representative coexistent attractors will have such a complicated basin boundary structure. The orange region is the basin of attraction for attractors at infinity which shows the coexistence of multiple attractors. In the yellow region, there is a line composed of a number of green points which fall in the center of the yellow region. They are the local minima points of Lyapunov exponential function, which indicate the stable points in phase space. They are also the solutions of a chaotic system, as well as the symmetry points of the basin of attraction. The blue region is the transitional region. From the basin of attraction diagrams for different orders, the basin of attraction section is a series of symmetric graphs which are unevenly distributed but have a self-similar appearance. From Figures 9–11 , we can see that system (1) has quite a few coexistent attractors. The basin of attraction is described by the Lyapunov exponent, so in the matlab program, we found the local minimum of the Lyapunov exponent. The green line was actually discrete points, but the figure was shrunk, making them look like a line. In the global basin of attraction figure, it can be found that the steady-state regions represented by yellow are spaced apart. So, they are multistable. Under different orders, the basin of attraction of system (1) shows different states, especially its area in the yellow region. How to use the radius of attraction to derive the size of a basin of attraction is a future field of concern. Now, that we have derived the position of the central point of the basin of attraction, the next step will be to obtain the size of the basin of attraction. Panorama of the base of attraction of system (1) with $q = 0.9$, as shown in Figure 12.

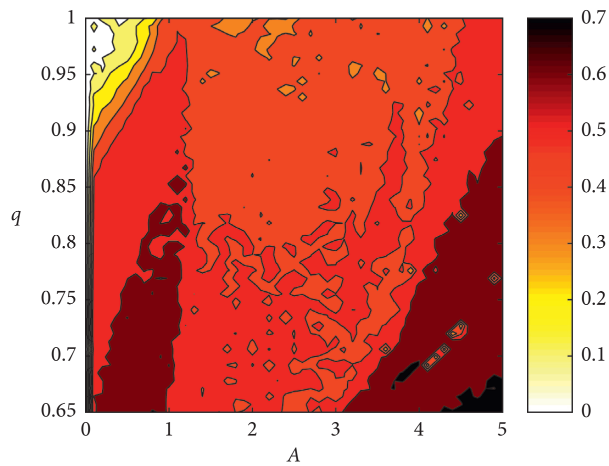

Figure 8: Chaos diagrams of fractional-order chaotic system (1): q-A plane.

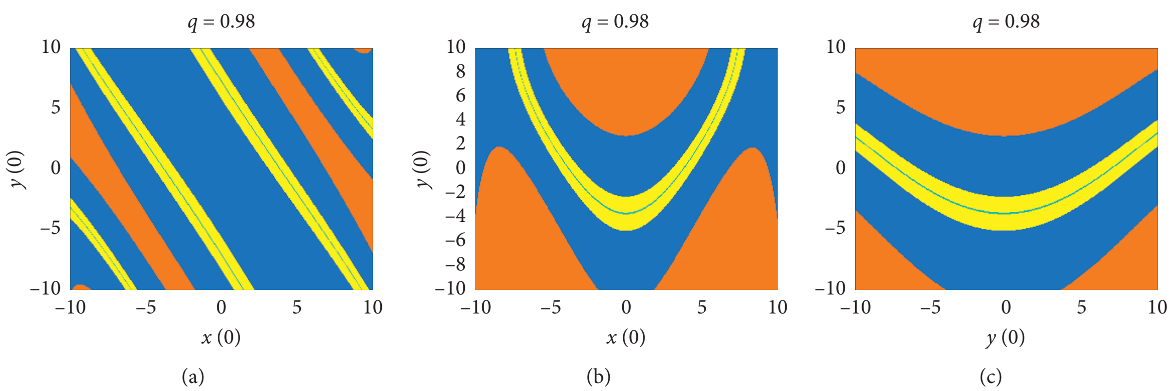

Figure 9: The basin of attraction of system (1) with $q = 0.98$: (a) $x(0)$–$y(0)$ plane, (b) $x(0)$–$z(0)$ plane, and (c) y (0)–$z(0)$ plane.

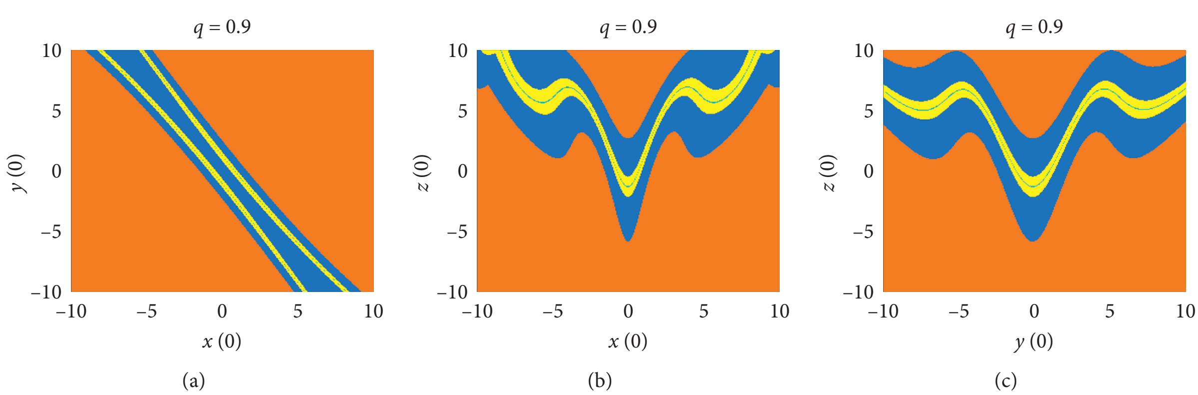

Figure 10: The basin of attraction of system (1) with $q = 0.9$: (a) $x(0)$–$y(0)$ plane, (b) $x(0)$-$z(0)$ plane, and (c) $y(0)$–$z(0)$ plane.

2.5. FPGA Implementation. The hardware experiment of system (1) with $q = 0.98$ is conducted by the method of fixed-point number, based on FPGA technology. We use Xilinx Zynq-7000 series XC7Z020 FPGA chip and AN9767 dual-port parallel 14 bit digital to analog conversion module with the maximum conversion rate of 125 MHz and adopt Vivado17.4 and the System Generator to realize the joint debugging of matlab: FPGA. Besides, we use oscilloscope to visualize the analog output. After the analysis, synthesis and compilation of Vivado. To further confirm that the chaotic system (1) is correct, after confirming that the timing simulation results are correct, generate the bit file by Vivado and download the generated bit file to the FPGA development board, convert the output of FPGA into the analog signal using AN9767 digital analog converter, and then connect AN9767 digital analog converter to the oscilloscope to observe the phase diagram of system (1) attractor. The phase diagrams displayed by the oscilloscope are, respectively, shown in Figure 13.

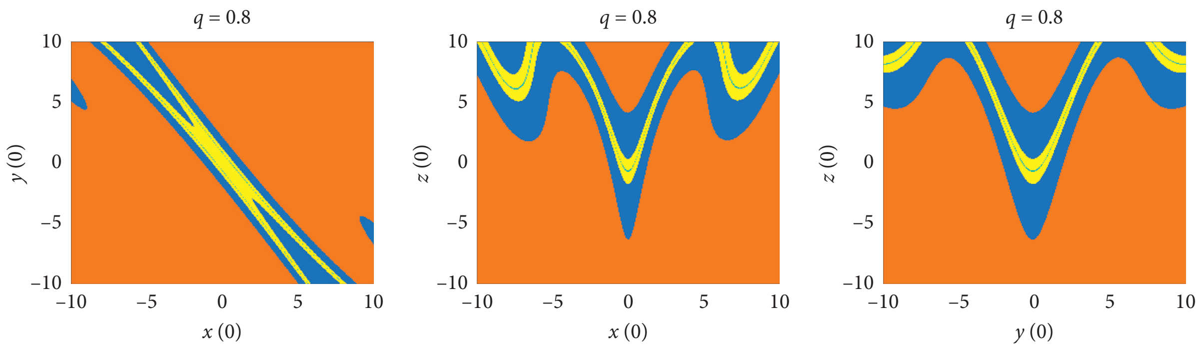

(a) (b) (c)

FIGURE 11: The basin of attraction of system (1) with $q = 0.8$: (a) $x(0)$–$y(0)$ plane, (b) $x(0)$–$z(0)$ plane, and (c) $y(0)$–$z(0)$ plane.

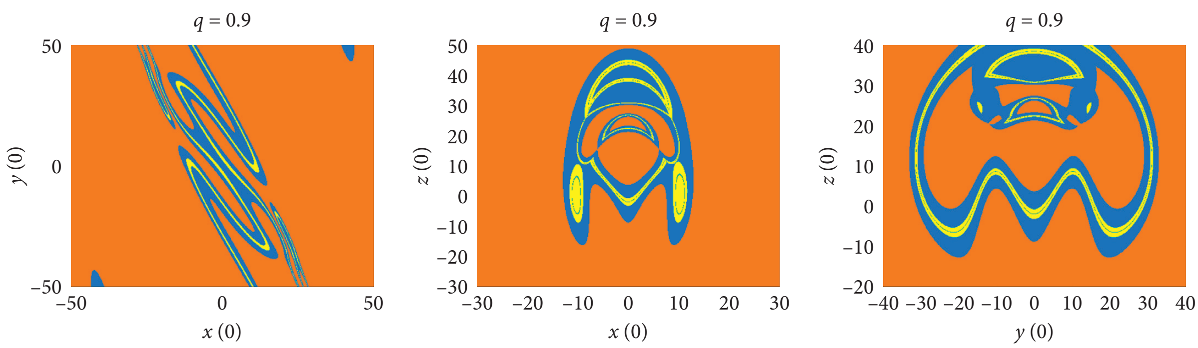

(a) (b) (c)

FIGURE 12: Panorama of the basin of attraction of system (1) with $q = 0.9$: (a) $x(0)$–$y(0)$ plane, (b) $x(0)$–$z(0)$ plane, and (c) $y(0)$–$z(0)$ plane.


(a) (b) (c)

FIGURE 13: The chaotic attractor of system (1) with $q = 0.98$. (a) x-y plane, (b) x-z plane, and (c) y-z plane.

3. Conclusions

Through the example of the memristor-based fractional-order chaotic system, this paper proposes a method to analyze the domain of attraction of the chaotic system via Lyapunov exponents. This method is used to depict the states when the orbit of the Lyapunov exponents takes different initial values, then obtain the center point of the attraction domain, and analyze the various states of the chaotic system as described under the domain of attraction at different orders. At the same time, the chaotic phase portraits are achieved by the solution of the proposed fractional-order chaotic system based on Adomian algorithm, and the dynamic analysis of the chaotic system is studied, such as

Lyaponov exponential spectrum, bifurcation, and SE complexity. Furthermore, this paper forecasts the future research directions and application areas of the domain of attraction.

Data Availability

The data used to support the findings of this study are included within the article.

Conflicts of Interest

The authors declare that they have no conflicts of interest.

Acknowledgments

This work was supported by the National Natural Science Foundation of China under Grant 61504013, Natural Science Foundation of Hunan Province under Grants 2019JJ50648 and 2020JJ4315, and Research Foundation of Education Bureau of Hunan Province.

References

[1] Z. Wen, Z. Li, and X. Li, "Transient MMOs in memristive chaotic system via tiny perturbation," *Electronics Letters*, vol. 56, no. 2, pp. 78–80, 2020.

[2] C. Wang, H. Xia, and L. Zhou, "A memristive hyperchaotic multiscroll jerk system with controllable scroll numbers," *International Journal of Bifurcation and Chaos*, vol. 27, no. 6, Article ID 1750091, 2017.

[3] S. Zhong, "Heterogeneous memristive models design and its application in information security," *Computers, Materials & Continua*, vol. 60, no. 2, pp. 465–479, 2019.

[4] M. Zhu, C. Wang, Q. Deng et al., "Locally active memristor with three coexisting pinched hysteresis loops and its emulator circuit," *International Journal of Bifurcation and Chaos*, vol. 30, no. 13, Article ID 2050184, 2020.

[5] X. Chen, S. Qian, F. Yu et al., "Pseudorandom number generator based on three kinds of four-wing memristive hyperchaotic system and its application in image encryption," *Complexity*, vol. 2020, Article ID 8274685, 17 pages, 2020.

[6] F. Yu, S. Qian, X. Chen et al., "Chaos-based engineering applications with a 6D memristive multistable hyperchaotic system and a 2D SF-SIMM hyperchaotic map," *Complexity*, vol. 2021, Article ID 6683284, 21 pages, 2021.

[7] F. Yu, S. Qian, X. Chen et al., "A new 4D four-wing memristive hyperchaotic system: dynamical analysis, electronic circuit design, shape synchronization and secure communication," *International Journal of Bifurcation and Chaos*, vol. 30, no. 10, Article ID 2050147, 2020.

[8] Y. Li, Z. Li, M. Ma, and M. Wang, "Generation of grid multi-wing chaotic attractors and its application in video secure communication system," *Multimedia Tools and Applications*, vol. 79, no. 39-40, pp. 29161–29177, 2020.

[9] F. Yu, Z. Zhang, L. Liu et al., "Secure communication scheme based on a new 5D multistable four-wing memristive hyperchaotic system with disturbance inputs," *Complexity*, vol. 2020, Article ID 5859273, 2020.

[10] B. Lu, F. Liu, X. Ge, and Z. Li, "Cryptanalysis and improvement of a chaotic map-control-based and the plain image-related cryptosystem," *Computers, Materials & Continua*, vol. 61, no. 2, pp. 687–699, 2019.

[11] H. Lin, C. Wang, F. Yu et al., "An extremely simple multi-wing chaotic system: dynamics analysis, encryption application and hardware implementation," *IEEE Transactions on Industrial Electronics*, vol. 1, 2021.

[12] J. Zeng and C. H. Wang, "A novel hyper-chaotic image encryption system based on particle swarm optimization algorithm and cellular automata," *Security and Communication Networks*, vol. 2021, Article ID 6675565, 10 pages, 2021.

[13] J. Liu, J. Li, J. Cheng et al., "A novel robust watermarking algorithm for encrypted medical image based on dtcwt-dct and chaotic map," *Computers, Materials & Continua*, vol. 61, no. 2, pp. 889–910, 2019.

[14] J. Deng, M. Zhou, C. Wang, S. Wang, and C. Xu, "Image segmentation encryption algorithm with chaotic sequence generation participated by cipher and multi-feedback loops," *Multimedia Tools and Applications*, vol. 18, 2021.

[15] W. Yao, C. Wang, Y. Sun et al., "Exponential multistability of memristive Cohen-Grossberg neural networks with stochastic parameter perturbations," *Applied Mathematics and Computation*, vol. 386, Article ID 125483, 2020.

[16] H. Lin, C. Wang, Y. Sun, and W. Yao, "Firing multistability in a locally active memristive neuron model," *Nonlinear Dynamics*, vol. 100, no. 4, pp. 3667–3683, 2020.

[17] T. Chen, L. Wang, and S. Duan, "Implementation of circuit for reconfigurable memristive chaotic neural network and its application in associative memory," *Neurocomputing*, vol. 380, pp. 36–42, 2020.

[18] H. Lin, C. Wang, W. Yao et al., "Chaotic dynamics in a neural network with different types of external stimuli," *Communications in Nonlinear Science and Numerical Simulation*, vol. 90, Article ID 105390, 2020.

[19] C. Ma, J. Mou, F. Yang et al., "A fractional-order hopfield neural network chaotic system and its circuit realization," *The European Physical Journal Plus*, vol. 135, no. 1, Article ID 100, 2020.

[20] H. Lin, C. Wang, Q. Hong, and Y. Sun, "A multi-stable memristor and its application in a neural network," *IEEE Transactions on Circuits and Systems II: Express Briefs*, vol. 67, no. 12, pp. 3472–3476, 2020.

[21] L. Chua, "Memristor-The missing circuit element," *IEEE Transactions on Circuit Theory*, vol. 18, no. 5, pp. 507–519, 1971.

[22] J. Sun, J. Han, P. Liu et al., "Memristor-based neural network circuit of pavlov associative memory with dual mode switching," *AEU-international Journal of Electronics and Communications*, vol. 129, Article ID 153552, 2021.

[23] Q. Lai, Z. Wan, P. D. K. Kuate et al., "Coexisting attractors, circuit implementation and synchronization control of a new chaotic system evolved from the simplest memristor chaotic circuit," *Communications in Nonlinear Science and Numerical Simulation*, vol. 89, Article ID 105341, 2020.

[24] Y. Peng, K. Sun, and S. He, "A discrete memristor model and its application in Hénon map," *Chaos, Solitons and Fractals*, vol. 137, Article ID 109873, 2020.

[25] C. Li, G. Chen, J. Kurths, T. Lei, and Z. Liu, "Dynamic transport: from bifurcation to multistability," *Communications in Nonlinear Science and Numerical Simulation*, vol. 95, Article ID 105600, 2021.

[26] Y. Shen and S. Zhu, "Multistability of delayed neural networks with monotonically nondecreasing linear activation function," *Neurocomputing*, vol. 423, pp. 89–97, 2021.

[27] Y. Zhang, Z. Liu, H. Wu, S. Chen, and B. Bao, "Two-memristor-based chaotic system and its extreme multistability

reconstitution via dimensionality reduction analysis," *Chaos, Solitons & Fractals*, vol. 127, pp. 354–363, 2019.

[28] A. Bayani, K. Rajagopal, A. J. M. Khalaf, S. Jafari, G. D. Leutcho, and J. Kengne, "Dynamical analysis of a new multistable chaotic system with hidden attractor: antimonotonicity, coexisting multiple attractors, and offset boosting," *Physics Letters A*, vol. 383, no. 13, pp. 1450–1456, 2019.

[29] F. Yu, L. Liu, H. Shen et al., "Multistability analysis, coexisting multiple attractors and FPGA implementation of Yu-Wang four-wing chaotic system," *Mathematical Problems in Engineering*, vol. 2020, Article ID 7530976, 2020.

[30] L. Qiu, W. Chen, F. Wang, and J. Lin, "A non-local structural derivative model for memristor," *Chaos, Solitons & Fractals*, vol. 126, pp. 169–177, 2019.

[31] A. S. Minhas, P. K. Kankar, N. Kumar, and S. Singh, "Bearing fault detection and recognition methodology based on weighted multiscale entropy approach," *Mechanical Systems and Signal Processing*, vol. 147, Article ID 107073, 2021.

[32] P. M. Cincotta, C. M. Giordano, R. A. Silva, and C. Beaugé, "The Shannon entropy: an efficient indicator of dynamical stability," *Physica D*, vol. 417, Article ID 132816, 2021.

[33] Z. Yuan, H. Chen, T. Li et al., "Fuzzy information entropy-based adaptive approach for hybrid feature outlier detection," *Fuzzy Sets and Systems*, vol. 54, 2020.

[34] P.-Y. Xiong, H. Jahanshahi, R. Alcaraz et al., "Spectral entropy analysis and synchronization of a multi-stable fractional-order chaotic system using a novel neural network-based chattering-free sliding mode technique," *Chaos, Solitons and Fractals*, vol. 144, Article ID 110576, 2021.

[35] L. Cui, M. Lu, Q. Ou et al., "Analysis and circuit implementation of fractional order multi-wing hidden attractors," *Chaos, Solitons and Fractals*, vol. 138, Article ID 109894, 2020.

[36] L. Cui, W.-H. Luo, and Q. Ou, "Analysis and implementation of new fractional-order multi-scroll hidden attractors," *Chinese Physics B*, vol. 30, no. 2, Article ID 020501, 2021.